ENGINEERING MODELS FOR THE MARS ATMOSPHERE BASED ON RECENT MEASUREMENTS OF MARS PATHFINDER AND MARS GLOBAL SURVEYOR

B. Petropoulos[1], P. Preka-Papadema[2] and G. Kiriakidis[b]

[1]Research Center for Astronomy and Applied Mathematics, Academy of Athens, Greece
[2]Section of Astrophysics, Astronomy and Mechanics, Dept. of Physics, University of Athens, Panepistimiopolis Zografos, Athens, Greece. E-mail: ppreka@cc.uoa.gr

ABSTRACT

Engineering models have been computed for the Mars atmosphere, from 0 to 120 km altitude. Physical parameters of temperature, pressure, density, number density, pressure scale, density scale, speed of sound, viscosity, collision frequency, mean collision velocity, mean free path and column mass have been computed, by internal of 1 km. The distribution of temperature measured by Mars Pathfinder and Mars Global Surveyor have been used as data for the computation of the above two different models. In order to compute these parameters, we have assumed that Mars atmosphere is in hydrostatic equilibrium. The perfect gas equation has been admitted, and we have resolved the hydrostatical differential equation. The computed physical parameters can be used for meteorological and engineering applications.

1. INTRODUCTION

The Mars Pathfinder (MP) and the MGS (Mars Global Surveyor) were the first among a long series of Mars exploration missions which have marked the return to Mars after the Viking missions (1976). The orbiter MGS arrived at Mars almost simultaneously with the MP Lander (1997), since its exploration program began in 1999 and continued until the end 2001. The surface temperature and pressure presents daily and seasonal variations according to all mission data. The MP and Viking missions as well as the MGS spectroscopic analysis at CO_2 spectral emission line of 15 _m recorded the temperature distribution vs altitude. A significant temperature difference between the layers near to the surface and the ones laid above them is presented. The thermal streamers due to intense atmospheric instability are conducted small or large dust clouds, the particles of which absorb the solar radiation and increase the opacity; as a result significant density variations are observed. The influence of dust on the energetic and heating equilibrium is an open question. Moreover, an anti-correlation between the presence of dust and the one of water-ice clouds is observed. The daily and seasonal variations are associated with dynamic phenomena, the solar radiation and the almost continue presentation of dust in the Martian atmosphere. For the above, details are given on http://mars.jpl.nasa.gov

Reference [7] presented a model to compute the physical parameters of the Martian atmosphere based on the Mariner 6 and 7 data and solving the hydrostatic equation taking into account the equation of ideal gases. This model applied on the Mariner 9 [5] and the Vikings 1 and 2 [8] observations in order to obtain the atmospheric parameters vs. altitude. In this paper, a new model of computation based on the MP and MGS data is presented. The results are compared with the ones of [8] to study the variations of physical parameters which is important to understand the seasonal variations, the role of dust clouds and the zonal winds behavior in the Martian atmosphere.

2. DATA COLLECTION AND COMPUTATIONAL RESULTS

The equation of ideal gases describe satisfactory the thin Martian atmosphere and their physical parameters are computed assuming the validity of hydrostatic equilibrium. The measurements of the surface pressure and the surface temperature as well as the distribution of the temperature vs. altitude (fig. 1) observed by MP and MGS missions [3], [1], [4], [2] are used in order to compute the most of the atmospheric parameters by interval of 1 km, until to about 120 km above the surface. The chemical composition of the Martian atmosphere (94.8 % CO_2, 3 % N_2, 2 % Ar^{40}, 0.2 % O_2 and Xe, Ne, He etc in smallest percentages) and the distribution of molecular weigh vs. altitude [6], [9] are assumed to have

remained as they were in the Viking missions. The following physical parameters of the atmosphere are obtained:

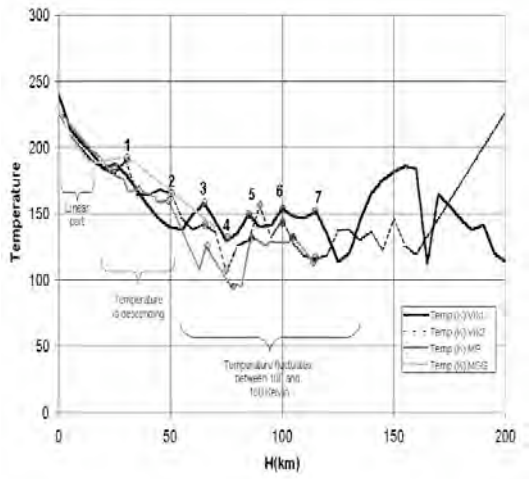

Fig.1. The temperature distribution vs. altitude recorded by the missions of MP (1997), MGS (1997), Viking1 (1976) and Viking 2 (1976). It shows a linear decrease until the altitude of 20 km, which continues with small fluctuations between 20 km and 60-70 km and some local minima and maxima in a range of 100-150 K, above the height of 60-70 km until 120 km. These fluctuations (pointed with numbers) have remained stable independently to the exploration mission data, while the gradients are more or less steep.

pressure, density, scale pressure, scale density, number density, and speed of sound, mean free path, mean particle velocity, collision frequency, coefficient of viscosity and columnar mass. Samples of the results are given in fig. 2, fig. 3 and fig. 4.

The computed results based on the MP data are compared with the ones of the Viking 1 because both of them arrived on Mars during the summer time and due to their neighboring with the landing sites (19.17 N, 33.21 W and 22.08 N, 48 W respectively). The surface temperature observed by MP and Viking1 was about 228 K and 239 K, while the surface pressure was 6.67 mb and 7.64 mb respectively. The temperature distribution vs. altitude is observed by orbiter MGS over the surface area with coordinates 52 N 290W, which is near to the Viking 2 landing site (48N, 226W). Although the MGS and Viking 2 measurements are received in different seasons of the Martian year (autumn and summer

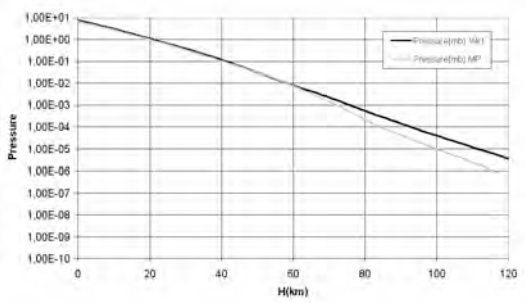

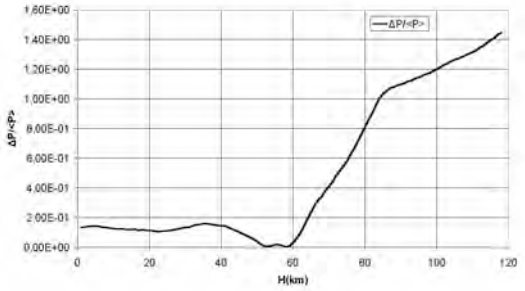

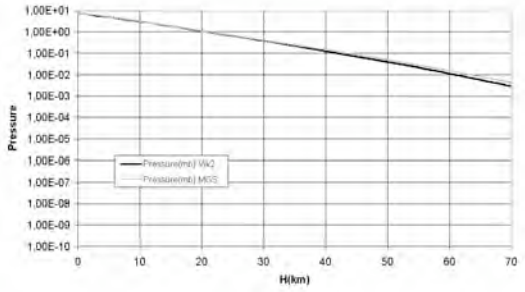

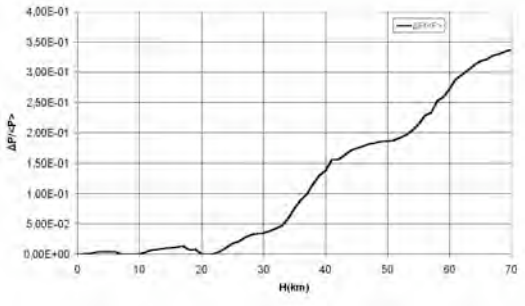

Fig. 2. The computed pressure distribution vs. altitude based on the MP and MGS data compared with the ones of Vikings 1 and 2 missions. A logarithmic decrease occurs, with identification between the MP and Viking 1 as well as MGS and Viking 2 results, in the lower altitudes. The computed values of MP in the upper layers (above 60 km) are smaller than the ones of Viking 1 and the difference increases with the altitude.

respectively), the temperature at an altitude of just 1 km above the surface recorded by MGS was 225 K, very similar to the surface temperature observed by Viking 2 (225.6 K). Consequently, the surface temperature and surface pressure (7.82 mb) observed by Viking 2 are used for the MGS model computation.

The distribution of temperature vs. altitude observed by MP and MGS as well as Viking 1 and 2 missions is shown in fig. 1. The MP observed values cover the height of 0-117 km and the MGS ones the height of 1-70 km. An almost linear decrease with gradient of -2.1 ± 0.5 K/km is obtained from all the four mission data, below 20 km. The decrease is continued between 20 km and 56 km with two local increases (pointed with numbers 1 and 2) at the height of 25-31 km and 49-52 km. The only small fluctuation observed by MGS is the one of the height of 31 km while a linear decrease with a gradient of -1.36 K/km is recorded upper than 31 km. The temperature between the altitudes of 56 km and 136 km is fluctuated in a range of 100-150 K with local minima (points 4 and 7) and local maxima (points 3, 5, 6) observed at the height of 63-68, 74-81, 85-91, 99-107 and 108-117 km. It is noticeable that all these small fluctuations are presented in the same height independently of the exploration mission which means they are stable in time. Although the Viking 2 measurements received during summer time and the ones of MGS during autumn, the Viking 2 values appeared slightly smaller than the ones of MGS, but the exact observed timing (day or night) is unknown for the MGS mission. Moreover, the MP observed temperatures above the height of 56 km were smaller and the gradients were larger (in same cases double) than the ones of Viking 1. It is noted that the MP landed after midnight while the Viking 1 after noon.

The computed pressure vs. altitude decrease logarithmically (fig. 2). It is noticeable that, there is identification between the MP and Viking 1 as well as MGS and Viking 2 results, until the altitude of about 60 km. The differences are smaller than 10% for the heights lower than 37 km and 10-35% for the ones between 37 km and 70 km, according to MGS and Viking 2 results, with the MGS values to be slightly larger than the Viking 2 ones. Above the 60 km and until 117 km, the computed pressure values based on the MP data are smaller than the ones of Viking 1 data. It seems that the difference increases with

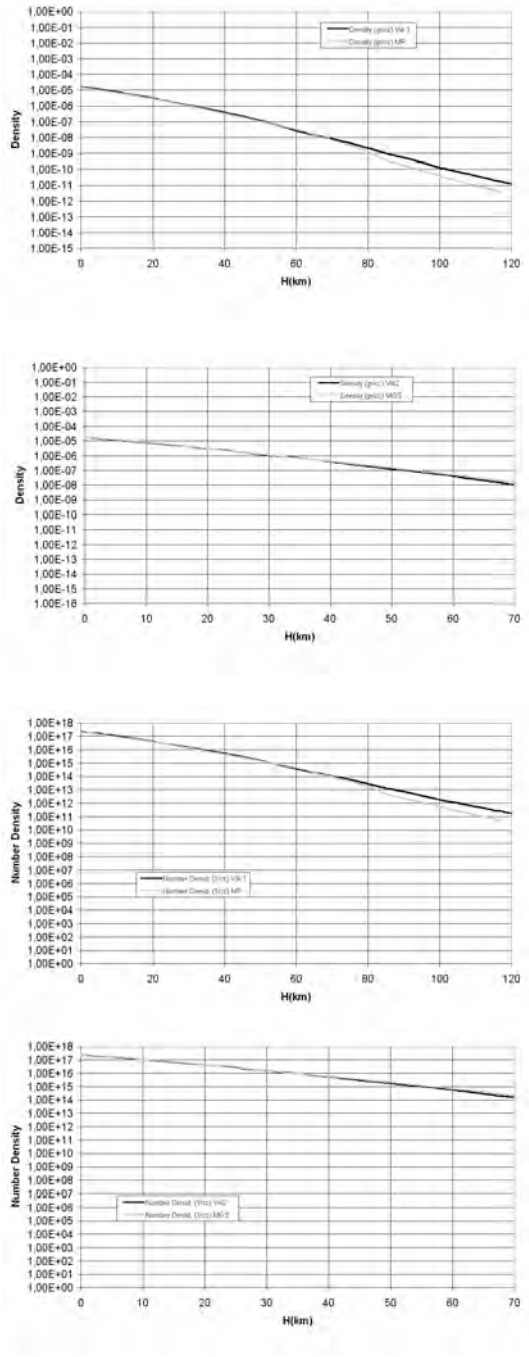

Fig. 3. The computed density and the number density distribution appear a logarithmical decrease vs. altitude which is similar to the one of pressure distribution (see fig. 2).

the altitude. Probably, there is some kind of relation between the pressure behavior and the smaller temperature with strong gradients recorded by MP in these atmospheric layers.

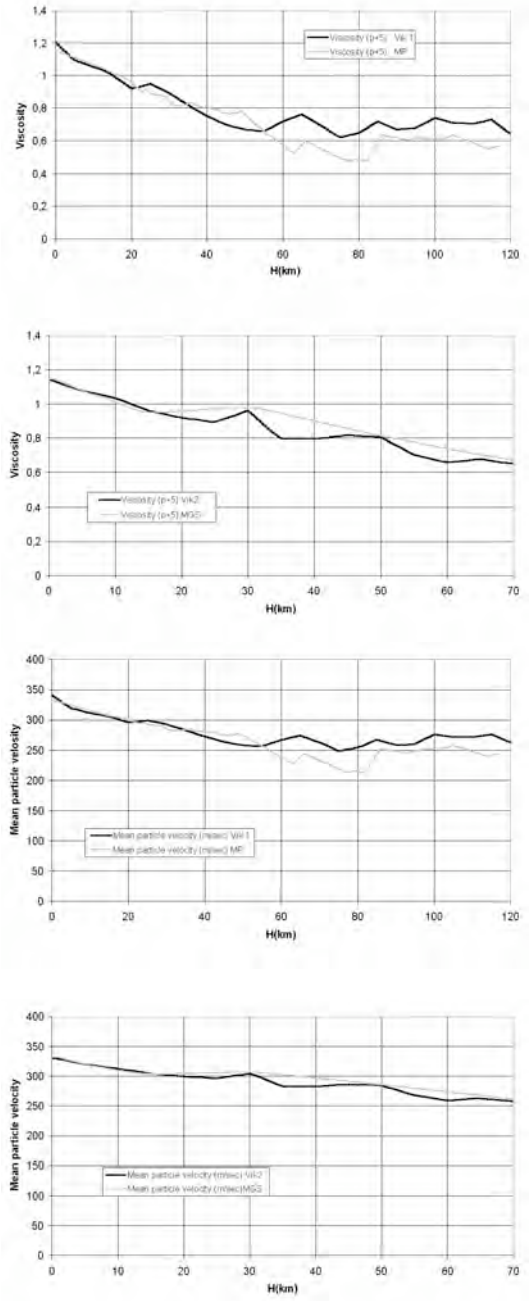

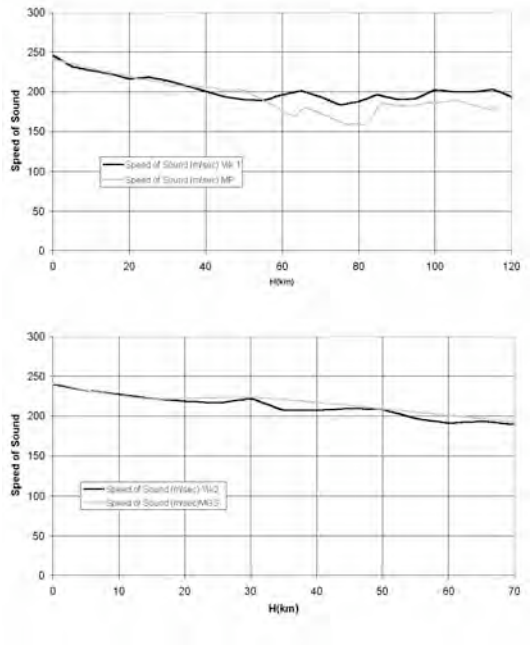

Fig. 4. The computed distribution of the coefficient of viscosity, speed of sound and mean particle velocity vs. altitude seem to follow the behavior of the temperature (see fig. 1).

Also, the computed density, number density and collision frequency appear a logarithmical decrease vs. altitude (fig.3), with identification below 60-70 km based on all the four mission data and a significant differentiation upper the 70 km with the MP values to be smaller than the ones of Viking 1. It seems that the logarithmical decrease of pressure determined the behavior of these physical parameters more than the distribution of temperature. For the same reason, the mean free path distribution increases logarithmically vs. altitude. In the contrary, the computed pressure scale, density scale, coefficient of viscosity, speed of sound and mean particle velocity seem to follow the behavior of the temperature vs. altitude (fig. 4). The columnar mass increases rapidly until 30 km and after a slowly increase until 60 km remains constant in the upper layers according to all four missions data. All the above presented results are available by the authors

3. CONCLUSIONS

Our results summarize as following: The pressure, density, number density and collision frequency decrease and mean free path increases logarithmically vs. altitude. It is note that, the

computed values based on different mission data do not present significant differences, until the altitude of about 60 km. This difference increases to the upper layers.

The coefficient of viscosity, speed of sound, mean particle velocity, pressure scale and density scale decrease vs. altitude in the lower layers, according to the temperature behavior. The observed temperature distribution appeared a linear decrease until the altitude of 20 km, which continued with small fluctuations between 20 km and 60 km and some local minima and maxima in a range of 100-150 K, above the height of 60 km until 120 km. It is noticeable that, despite the gradients are more or less steep; these fluctuations have remained stable independently to exploration mission data.

Probably, the pressure distribution between 60 km and 120 km is associated with the temperature distribution, with its smaller values and strong gradients corresponded to the smaller pressure values. The density, number density and collision frequency distribution are followed the pressure behavior.

The thermodynamic equilibrium is valid in the lower Martian atmosphere (<100 km) while the upper layers influenced by the variations of the photochemical reactions which depend on the solar radiation. The recent missions of Mars Odyssey (2001), Mars Express (2004), Spirit (2004) and Opportunity (2004) arrived on Mars during the maximum of solar activity, while the previous ones of Viking 1 and 2 (1976), MP (1997) and MGS (1997) near the solar minimum. Similar model computations using data from the recent missions and comparing them with these results should give useful information to study climatic variations. It is very important to understand the behavior of physical parameters, the structure and the mechanisms of the Martian atmosphere in order to improve the future plans of missions, especially the successfully landing with aero braking method.

4. REFERENCES

1. Bell J., *Sky and Telescope*, Vol. 96 (1), 36, 1998.
2.Christensen P. R., Anderson D. L., Chase S. C., et al, *Science*, Vol. 279, 1696, 1998.
3. Goldman S. J., *Sky and Telescope*, Vol. 94 (5), 32, 1997.
4. Kahn R., *Sky and Telescope*, Vol. 94 (4), 38, 1997.
5. Makris K. and Petropoulos B., *Com. Rend. Acad. Sci*., Vol. 39, 1977.
6. Owen T. and Biermann K., *Science*, Vol. 193, 801, 1976.
7. Petropoulos B., *Doc. Es.Sci.Phys*., Paris, France, 1974.
8. Petropoulos B. and Makris K., *Earth, Moon and Planets*, Vol. 46,1, 1989.
9. Seiff A. and Kirk D. B., *J. Geophys. Rev*., Vol. 30, 4364, 1977.